Performance of the cost-effective Planacon® MCP-PMTs in strong magnetic fields

Yu.A. Melikyan [a,*], I.G. Bearden [b], E.J. Garcia-Solis [c], V.A. Kaplin [d], T.L. Karavicheva [a], J.L. Klay [e], T. Marszał [f], I.V. Morozov [a], D.V. Serebryakov [a], M. Slupecki [g], W.H. Trzaska [h]

[a] *Institute for Nuclear Research of the Russian Academy of Sciences, V-312, 60-letiya Oktyabrya prospect 7a, Moscow, 117312, Russia*
[b] *Niels Bohr Institute, University of Copenhagen, Nørregade 10, 1017 Copenhagen, Denmark*
[c] *Chicago State University, 9501 S. King Drive, Chicago, IL 60628, United States*
[d] *National Research Nuclear University MEPhI (Moscow Engineering Physics Institute), Kashirskoe shosse 31, Moscow, 115409, Russia*
[e] *California Polytechnic State University, 1 Grand Avenue, San Luis Obispo, CA 93407, United States*
[f] *National Centre for Nuclear Research, 7 ul. Andrzeja Sołtana, 05-400 Otwock, Świerk, Poland*
[g] *Helsinki Institute of Physics, University of Helsinki, P.O. Box 64, FI-00014, Finland*
[h] *Department of Physics, University of Jyväskylä, P.O. Box 35 (YFL), FI-40014, Finland*

ARTICLE INFO

ABSTRACT

We present the behavior of the cost-effective Planacon MCP-PMTs with 25 μm pore diameter in the presence of axial magnetic fields up to 0.5 T. Having a batch of 62 devices of the same type, two MCP-PMTs were selected and their gain variation measured in different magnetic fields. These two otherwise identical devices satisfied the selection criteria by requiring the lowest (1.15 kV) and one of the highest (1.4 kV) bias voltage values to achieve a given gain. Both MCP-PMTs have a nearly identical tolerance of the strong magnetic field despite the significant difference in the bias voltage. This clarifies the mechanism of the B-field influence on the MCP-PMT gain, emphasizing the importance of the intrinsic parameters of the MCP emissive coating rather than external parameters, such as the total bias voltage. By evaluating the dependence of both gain and timing parameters on the magnetic field strength, we confirm the operability of such MCP-PMTs in strong magnetic fields in spite of the relatively large pore diameter and low bias voltage required for a given gain.

1. Introduction

Photomultiplier tubes based on microchannel plates (MCP-PMTs) are frequently used as active components of particle identification (PID) and trigger detectors in a wide range of modern accelerator-based experiments [1–6]. One of the main reasons limiting the application of other PMT types in such experiments is the use of strong magnetic fields. In particular, small-pore (≤ 6 μm) MCP-PMTs are considered to be nearly insensitive to strong magnetic fields of a magnetic flux density up to B$\approx$0.5 T [7]. One of the main drawbacks of these devices is a relatively high price resulting from a complicated manufacturing process. In the standard approach, it involves multiple steps of thermo-mechanical and chemical processing of thousands of lead glass fibers each reduced down to sub-mm dimensions of a single MCP pore. It makes the cost of large-pore MCPs significantly lower than small-pore MCPs of the same dimensions. For example, 25 μm-pore MCP-PMTs are the most cost-effective options of Planacon photosensors available from Photonis, Inc.

As a part of the R&D activities necessary for the Fast Interaction Trigger (FIT) detector for the upgraded ALICE apparatus at CERN [1,8],

we have selected and tested 25 μm-pore Planacon MCP-PMTs with 53×53 mm^2 sensitive area as the photosensors of choice for the FIT Cherenkov subsystem. To complete the project, we need 52 (+10 spare) PMTs to be operational at $1.5\cdot10^4$ electron gain in the magnetic field of the ALICE L3 solenoid magnet [1] (typically ±0.2 T or ±0.5 T). In the case of FIT, the low-gain operation is optimal to detect relativistic particles with the best timing in a wide range of particle flux values [9], keeping the devices in the linear operation mode. 62 Planacons for ALICE FIT were manufactured throughout 2018 and 2019. As we know from bench testing of these devices outside strong magnetic field, the total bias voltage requirements for the default electron gain ($1.5\cdot10^4$) vary from 1.15 kV to 1.4 kV. None of the available systematic studies of the MCP-PMT performance in strong magnetic fields present the data for such low bias voltage values [10–17]. However, the low-voltage operation of an MCP-PMT is beneficial from the point of the device lifetime, which is believed to be limited by the ion feedback, proportional to the voltage applied [18].

According to our preliminary study done for a single Planacon and reported before [9], placing the device biased to the gain of $1.5\cdot10^4$ in a

---

Table 1

Basic parameters of the two out of 62 MCP-PMTs produced for FIT.

Type	Photonis Planacon XP85002/FIT-Q	
Pore diameter	25 μm	
ALD-coating	no	
Sensitive area	53×53 mm^2	
Serial #	9 002 129	9 002 166
Alias	"High SEY"	"Low SEY"
MCP stack resistance at $U_b = 1400$ V	14.7 MΩ	15.3 MΩ
U_b for $1.5 \cdot 10^4$ gain	1155 V	1394 V
U_b for 10^6 gain	1485 V	1797 V

0.5 T magnetic field results in a decrease in gain by a factor of 2.5. This reasonably small value was only measured for the total bias voltage of 1.35 kV, so this limited study is insufficient to predict the operability of any similar devices in a strong magnetic field. Testing the device at a lower bias voltage, e.g. 1.15 kV, has shown a decrease in gain by a factor of ∼8 [9]. Such a significant gain drop is undesirable for many applications, including for use in the ALICE FIT detector. However, for the device under discussion, the lower voltage of 1.15 kV corresponds to an electron gain of $6 \cdot 10^2$ only. Since the mechanism of the magnetic field influence on the MCP-PMT gain is not completely clear, these results may not be predictive for most applications which require the device to operate at a much higher gain.

To make sure that all of the new cost-effective Planacon MCP-PMTs are operable in a strong magnetic field, we have measured and compared the dependence of gain on the magnetic field for two MCP-PMTs selected from the batch production. These otherwise identical devices were selected from the extreme ends of the gain vs. voltage distribution (see Fig. 1 and the description below). Furthermore, we have quantified the voltage adjustments needed for each of the 62 MCP-PMTs produced for FIT to keep their gains in B = 0.2 T and B = 0.5 T magnetic fields the same as in B = 0 T.

2. Planacon XP85002/FIT-Q MCP-PMTs

To fulfill all FIT requirements for the detector granularity, timing, load capacity, and length, we have developed a custom backplane with 2×2 segmented anode readout and decided to use MCPs of a reduced resistance (12 MΩ ≤ R$_{MCP}$ ≤ 22 MΩ) [9]. Such modified Planacon MCP-PMTs acquired a dedicated model name XP85002/FIT-Q. Although the tested Planacons have been modified for the use with FIT, the modifications are not expected to influence the described behavior of the sensors in strong magnetic fields.

All 62 of the devices, mass-produced for ALICE FIT, have undergone an extensive bench testing procedure. While most of the bench testing results are beyond the scope of this article, we note that among the whole production consignment of 62 devices supplied in 9 separate batches, a significant spread in total bias voltage needed for a given electron gain was observed. For example, MCP-PMT #9002129 requires the lowest total bias voltage (U$_b$) for a given electron gain, while #9002166 requires one of the highest voltage values. Fig. 1 compares the gain curves of these two devices with those for the remaining 60 from tested production batch of MCP-PMTs.

For the tested devices, the electron gain is determined by measuring single photoelectron charge spectra (description of this technique could be found in [19]). Since the electron gain value is not affected by the collection efficiency, the observed difference of the bias voltage is caused by a different average secondary electron yield (SEY) of the inner coating of the MCP pores. Because of this and for the reader's convenience, below we refer to the devices #9002129 and #9002166 as "High SEY" and "Low SEY" respectively. Basic characteristics of these MCP-PMTs are listed in Table 1. The voltage divider circuit, we use for each tested device, is shown in Fig. 2.
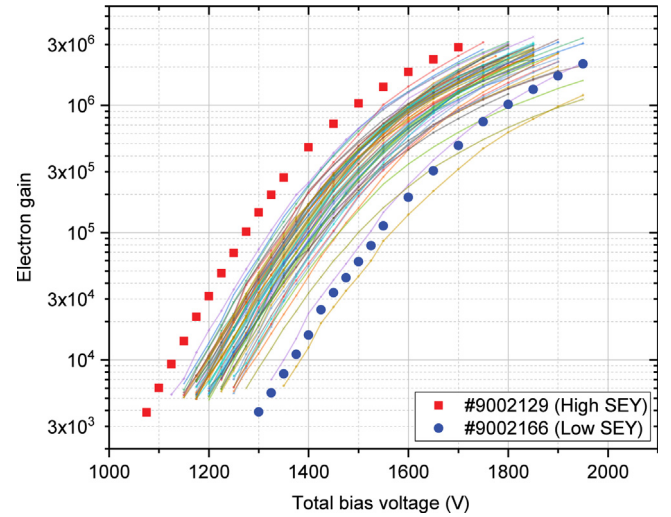

Fig. 1. Electron gain values as a function of the total bias voltage measured for the Planacon XP85002/FIT-Q MCP-PMTs #9002129 (High SEY) and #9002166 (Low SEY) in comparison to the same dependencies for the other 60 mass-produced devices.

3. Experimental set-up

The study was performed in the homogeneous (within ±0.5%) field region, sized $1.0 \times 0.5 \times 0.3$ m^3, of the 20-ton MNP17 dipole magnet at CERN. A schematic of the experimental set-up is shown in Fig. 3. The B-field value (magnetic flux density) was monitored by the Gauss/Tesla meter F.W. Bell 4048. Measurement of the properties of the Low SEY and High SEY MCP-PMTs was done by placing them in an individual light-tight housing with custom optical fiber inputs. The MCP-PMTs feature four square-shaped independent readout channels (quadrants) [9]. The first quadrant of each device was illuminated by 405 nm light produced by an optical pulse generator (Advanced Photonic Systems EIG1000D laser) and passed through an optical attenuator (OZ-optics DA-100) and an optical splitter. The width of the laser pulses was less than 45 ps, while the timing jitter is claimed by the manufacturer to be less than 3 ps. The laser light intensity was monitored and confirmed to be stable within 1% for the whole set of measurements done for each MCP-PMT with the help of a reference PMT (Philips 56 AVP) placed outside the magnet. The signals were digitized and their parameters measured by a LeCroy WaveRunner 8104 digital oscilloscope with 1 GHz bandwidth and 10 GS/s sampling rate.

4. B-field influence on the MCP-PMT response

Figs. 4 and 5 show in red the ratio of the signal amplitude at 0.5 T to the signal amplitude at 0 T and, in black, the ratio of the signal amplitude at 0.2 T to the signal amplitude at 0 T. In Fig. 4 both ratios are plotted as a function of the bias voltage, while in Fig. 5 – as a function of the electron gain at B = 0 T. The values for High SEY are rendered in deeper shades and connected by solid lines to guide the eye. The values for Low SEY are rendered as pale red and gray points connected by dashed lines to guide the eye. The measurements with the results presented in Figs. 4 and 5 were conducted with the magnetic field from 0 to 0.5 T varied gradually with 25...50 mT steps. The more complete data set on the variation of the signal amplitude at a given magnetic field relative to zero field ("Relative signal amplitude") is presented in Figs. 6 and 7. Fig. 6 data was obtained for total bias voltage values from 1.1 kV to 1.5 kV corresponding to electron gain values in the ranges $6 \cdot 10^3$–10^6 and $2 \cdot 10^2$–$5 \cdot 10^4$ for the high SEY and low SEY MCP-PMTs, respectively. The same data is re-plotted in Fig. 7 arranged by the MCP-PMT electron gain at B = 0 T. Electron gain values from $2 \cdot 10^2$ to 10^6 were achieved at total bias voltage values in the
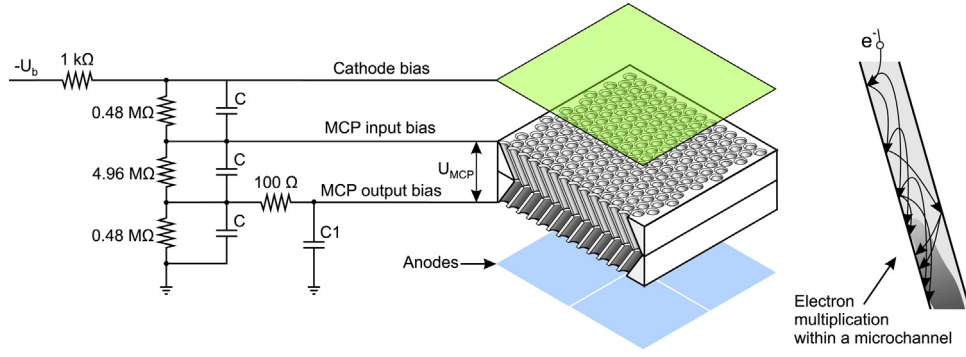
Fig. 2. The voltage divider circuit used for all tested Planacon MCP-PMTs. The picture also presents a simplified schematic and the operation principle of an MCP-PMT with a chevron MCP stack.
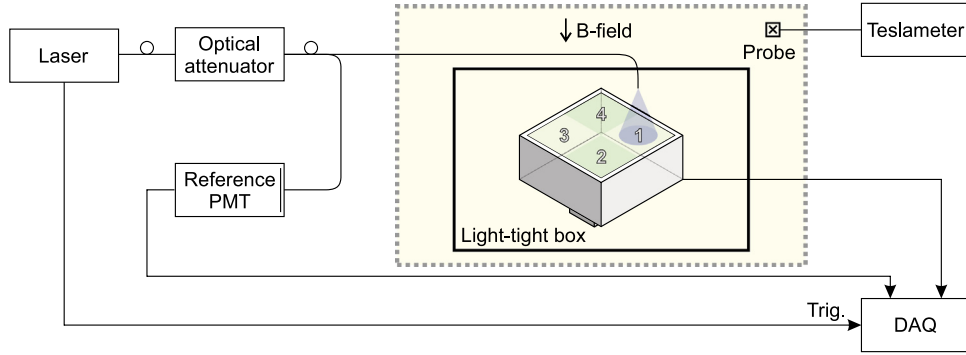

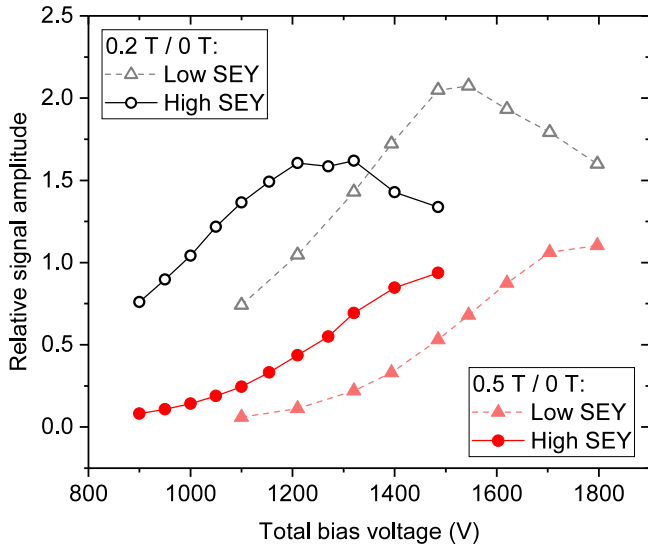**Fig. 3.** Schematic of the experimental set-up.

Fig. 4. MCP-PMT signal amplitude in B = 0.2 T and B = 0.5 T relative to B = 0 T magnetic field as a function of the total bias voltage. The lines connecting the points are drawn for visual purposes only.
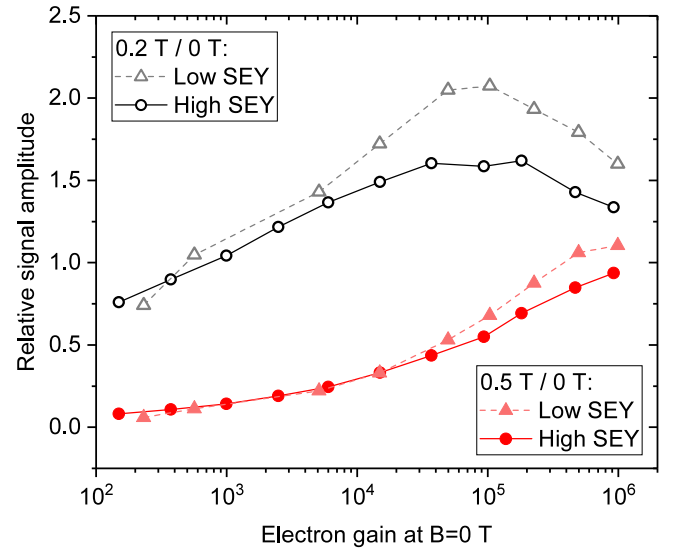
Fig. 5. MCP-PMT signal amplitude in B = 0.2 T and B = 0.5 T relative to B = 0 T magnetic field as a function of the electron gain value at B = 0 T. The lines connecting the points are drawn for visual purposes only.

range 0.9–1.5 kV and 1.1–1.8 kV for the High SEY and Low SEY MCP-PMTs, respectively. The full data set related to Figs. 6 and 7 is presented in the attachment to this manuscript.

Both devices require a very low total bias voltage compared to the MCP-PMTs of other manufacturers and earlier versions of Planacon MCP-PMTs [10,12,16,17,20]. However, the exact total bias voltage values for each device differ significantly among them, particularly considering their identical mechanical and very similar electrical characteristics. Moreover, as can be seen from Figs. 4 and 6, the response

of the two MCP-PMTs to the B-field variation is clearly different when biased to the same voltage, while it is rather similar when biased to an equal gain (Figs. 5 and 7). The two curves presenting the 0.5 T magnetic field influence to the signal amplitude in Fig. 5 overlap for the initial electron gain values from $5 \cdot 10^2$ to $5 \cdot 10^4$ within ±15%. In other words, influence of a strong magnetic field to the MCP-PMT gain is independent of the bias voltage value applied to the MCP. At the same time, it may depend on the other MCP-PMT parameter determining its gain at zero magnetic field — the average SEY of the MCP pores. This
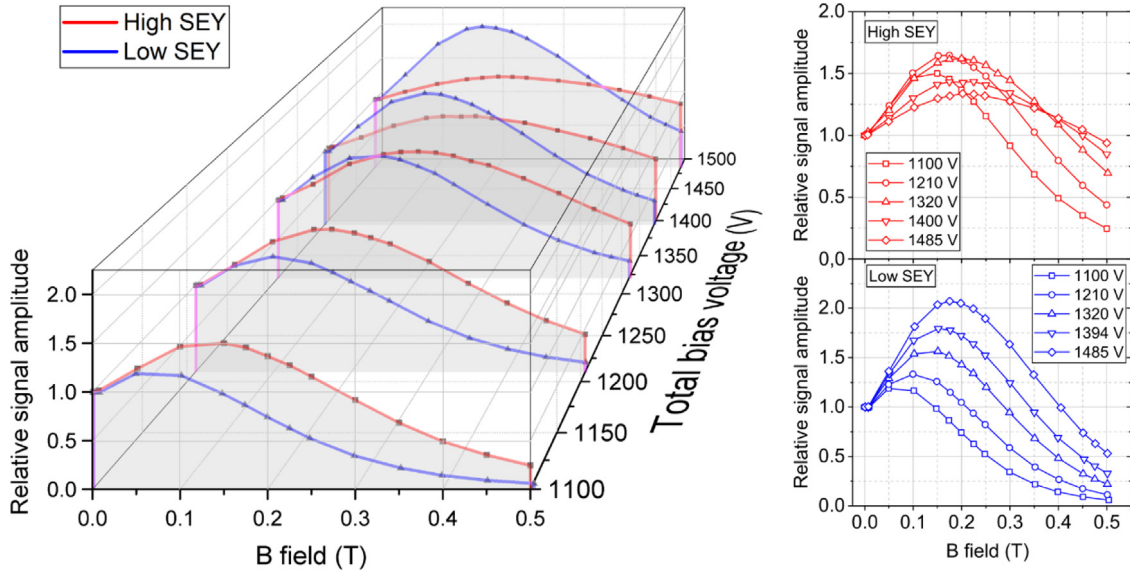
Fig. 6. MCP-PMT signal amplitude relative to B = 0 T case as a function of B-field strength for different bias voltages. The lines connecting the points are drawn for visual purposes only.
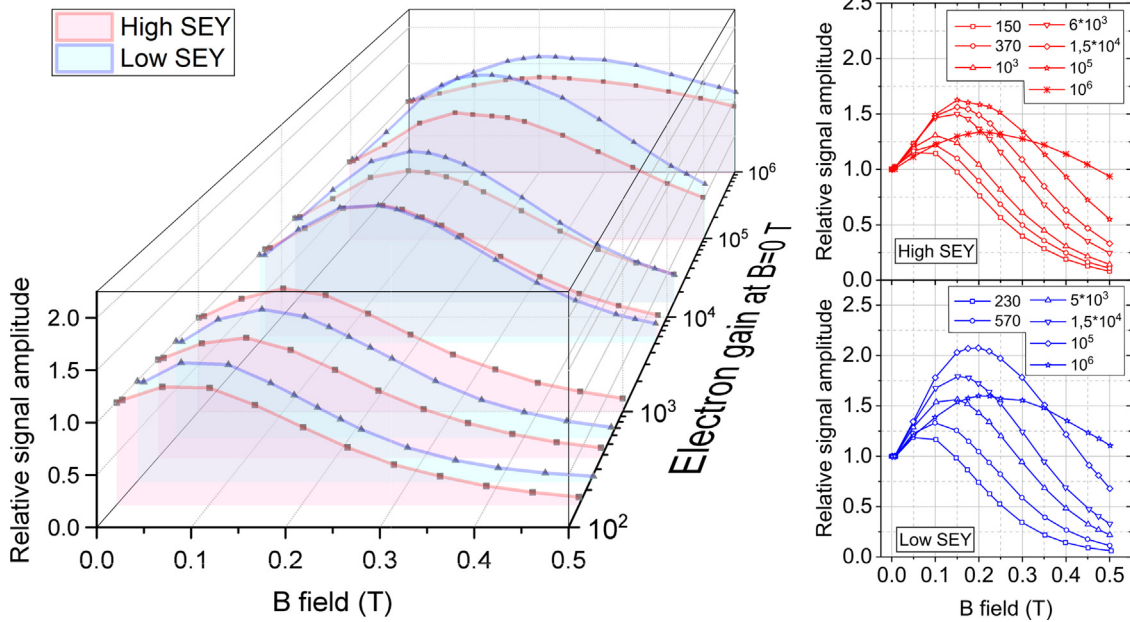

Fig. 7. MCP-PMT signal amplitude relative to the B = 0 T case as a function of B-field strength for different electron-gain values at B = 0 T. The lines connecting the points are drawn for visual purposes only.

indicates that the significant decrease in the total bias voltage needed for the modern Planacon MCP-PMTs to achieve a given gain does not seem to cause an extra drop in gain when using these devices in strong magnetic fields of up to B = 0.5 T.

This behavior is further supported by the results of brief testing of all 62 FIT MCP-PMTs in strong magnetic field as presented in Figs. 8 and 9. As one can see from Fig. 8, the effect of the 0.5 T magnetic field on the MCP-PMT response initially operating at $1.5 \cdot 10^4$ electron gain can be compensated by a relatively small increase in bias voltage of 50 to 80 V, while a decrease in total bias voltage of 10 to 40 V compensates for the effect of B = 0.2 T. Moreover, the data shows no sign of an inverse dependence between the absolute values of the compensatory voltage and the total bias voltage (needed for the device to achieve the default gain at B = 0 T). This is true both for the bias compensation dependencies on the total bias voltage (Fig. 8), and

on the voltage across the MCP (Fig. 9) – the proportionality between these two parameters is broken by the spread in the MCP resistance mentioned above (12 MΩ ≤ R_{MCP} ≤ 22 MΩ). No inverse dependence observed in Figs. 8 and 9 brings hope that those MCP-PMTs with even lower bias voltage (due to even higher SEY) may require bias compensation comparable to those values measured for the devices under study.

The data presented so far is from measurements for which the B-field direction was oriented opposite to the Planacon's line of sight (as indicated in Fig. 3), even though MCP-PMTs are typically operated within detectors for which magnetic field of both directions is used, including the ALICE FIT [1–6]. To make sure the obtained results are relevant for both B-field orientations, the signal amplitude and timing parameters of the Planacon #9002166 were measured performing an upside-down rotation of the PMT housing to alternate the mutual
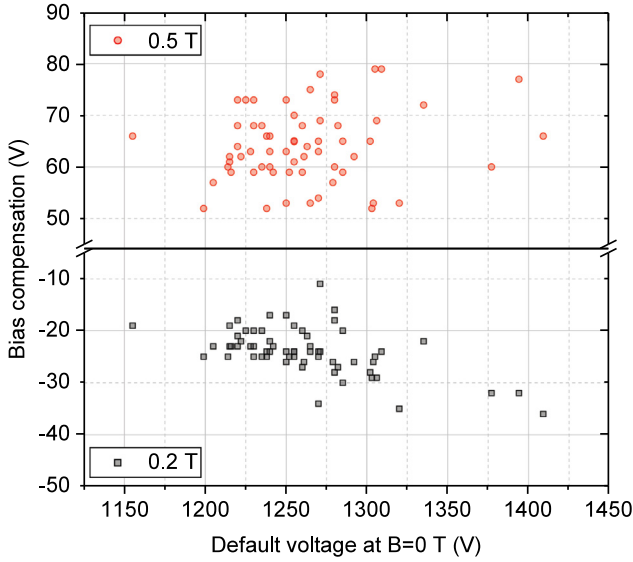
Fig. 8. Voltage correction needed to restore the initial electron gain of $1.5 \cdot 10^4$ after introducing Planacons to 0.2 T and 0.5 T B-field.
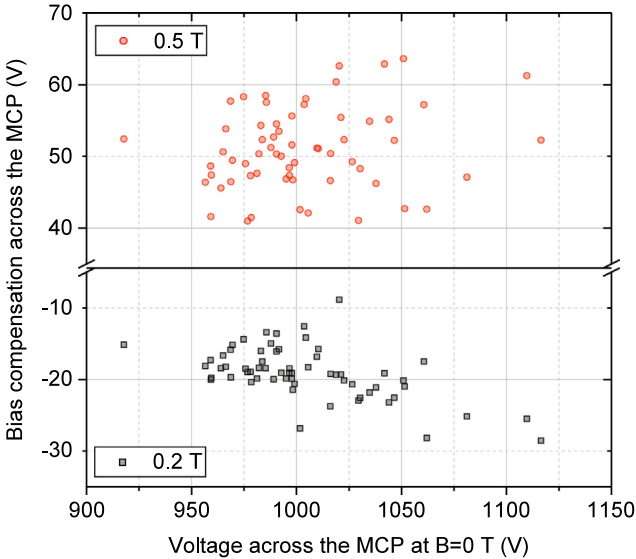

Fig. 9. The same values, as in Fig. 8, but recalculated to the voltage values across the MCP stack only.

orientation of the MCP-PMT and the magnetic field. The results are presented in Figs. 10 and 11, showing an identical (within ±4%) Planacon performance in axial magnetic fields of opposite directions. The minor mismatch of the curves may arise from measurement uncertainty caused by the rotation of the PMT housing, although this uncertainty was not estimated quantitatively.

The data for Figs. 10 and 11 was obtained with a single set of measurements. The arrival time spectra of the MCP-PMT anode signals were measured with a software-based CFD implemented in the LeCroy WR8104 oscilloscope. The CFD algorithm was set to trigger at the 50% fraction of the pulse amplitude. The arrival time spectra were fitted with a Gaussian function determining the mean and sigma values. The former value represents the time delay, which, according to Fig. 11, may reach 0.3–0.5 ns at 0.5 T magnetic field. The latter value represents the time resolution. In order to keep the MCP-PMT output in linear mode [21,22], each pair of curves was measured at a different pulse intensity: $3 \cdot 10^5 - 10^2$ photoelectrons per readout channel for 1210 V– 1797 V total bias voltage, respectively. Under such conditions, the

average time resolution was measured to be $\sigma = 12 \pm 3$ ps including the contribution of the laser pulse generator (defined in Section 3), and no significant variation in this value was observed over the range of B-field values applied.

5. Discussion

A set of publications describes the behavior of the MCP-PMTs (including those of the Planacon type) biased to 1.8...3.5 kV in magnetic fields up to 4.5 T [10–17,20,23,24], but any information for bias voltage values under 1.8 kV is missing from the literature. This lower voltage regime is particularly interesting due to the fact that modern MCP-PMTs can operate with unprecedentedly low total bias voltages down to $U_b = 1.15$ kV for $1.5 \cdot 10^4$ electron gain (920 V only across the MCP stack) or ~1.5 kV for 10^6 electron gain. To reach the same gain, other devices reported elsewhere require total bias voltage values higher by 500–1500 V.

Figs. 4 and 5 confirm the operability of the cost-effective Planacons biased to $1.5 \cdot 10^4$ electron gain under magnetic-field values relevant for the ALICE FIT even with total bias voltage down to 1.15 kV. Figs. 4 and 6 also shed more light on the influence of the magnetic field on the MCP-PMT gain. According to [13], this may be caused by the shrinkage of the electron spiral trajectories when the Larmor radius becomes comparable to the pore size, preventing the electrons from impinging the channel walls. If this were the case, one might expect an equal magnetic field influence on the performance of two devices with identical inner dimensions biased to an equal voltage. However, this is not true for the Low SEY and High SEY devices tested here.

Similar B-field influence on the performance of these two devices biased initially to the same gain (Fig. 7) conforms well with the mechanism described in [7] and [11]. In this assumption, the Lorentz force creates an additional curvature of electron trajectories, increasing the average number of their collisions with the pore walls, thus increasing the gain. When the kinetic energy of secondary electrons at the moment of collision becomes insufficient to pull out more than one electron, gain starts decreasing. Here, we note that the dependence of the secondary electron yield of the inner SiO_2 coating of Planacon pores [25,26] on the incoming electron kinetic energy exhibits a peak value at ~200 eV decreasing for both higher and lower electron energies [27]. Thus, the MCP-PMT gain in a strong magnetic field might likely be a trade-off between the average number of electron collisions and the average SEY, both having a non-obvious dependence on the B-field value. It is important to note, that the latter parameter becomes even more critical for the ALD-coated MCP-PMTs [28] because of a much steeper dependence of the average SEY on the electron kinetic energy [27].

The previous discussion should be kept in mind when identifying the optimal MCP-PMT photosensor for given experimental conditions from the point of cost and performance in strong magnetic fields. Different attempts have been made to develop a technique to simulate the parameters of certain MCP-PMT types in the magnetic field of a given direction and magnetic flux density [7,29,30]. Nevertheless, none of the available solutions were confirmed to be a universal tool matching any MCP-PMT type. We understand that the development of a universal simulation tool and the verification of its predictive power require many datasets on the magnetic field influence on the performance of different MCP-PMTs with well-known parameters. As our modest contribution to this task, we present here the dataset for the strong axial magnetic field influence on Planacon XP85002/FIT-Q MCP-PMTs. New data on the performance of these MCP-PMTs in non-axial magnetic fields and their saturation parameters is upcoming.
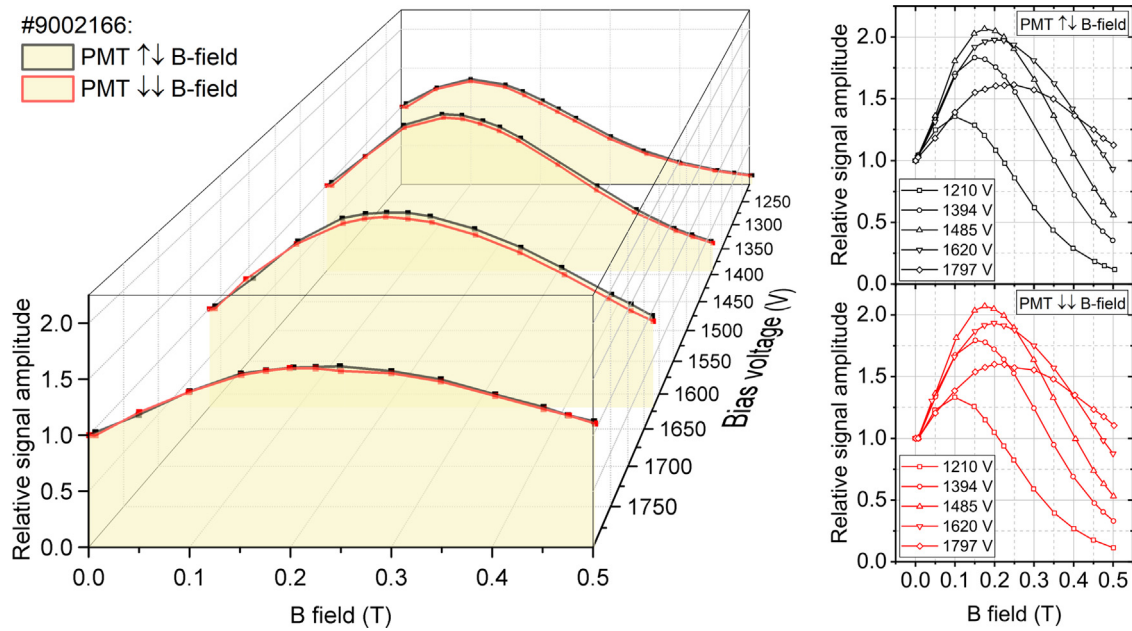
Fig. 10. MCP-PMT signal amplitude relative to the B = 0 T case as a function of B-field strength for different total bias voltage values and field orientations. Mutual orientation of the B-field direction and the MCP-PMT line of sight is indicated in the legend with arrows. The lines connecting the points are drawn for visual purposes only.
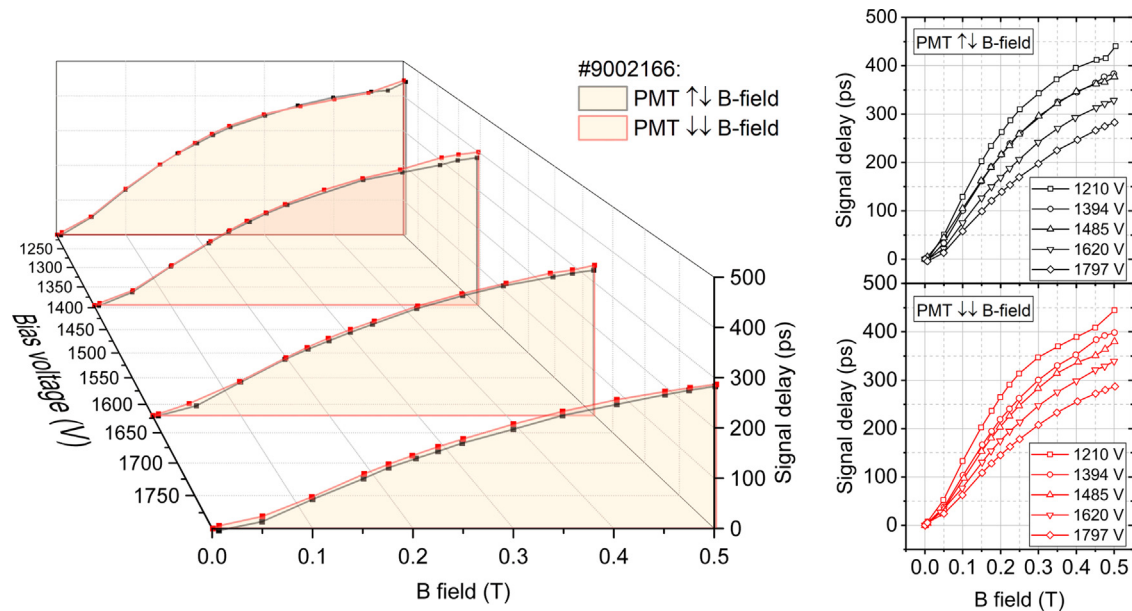
Fig. 11. Variation in the MCP-PMT signal propagation time as a function of B-field strength for different total bias voltage values and field orientations. Mutual orientation of the B-field direction and the MCP-PMT line of sight is indicated in the legend with arrows. The lines connecting the points are drawn for visual purposes only.

6. Conclusions

Modern 25 μm-pore Planacon MCP-PMTs require an unprecedent-edly low total bias voltage to achieve a given gain, which is very beneficial as this minimizes the level of afterpulsing and increases the device lifetime. Despite the relatively large pore size and low total bias voltage, the devices are operable in strong magnetic fields up to 0.5 T with only a moderate change in their response: signal amplitude may drop by a factor of 3 or rise by a factor of 2 at $1.5 \cdot 10^4$ initial gain. This behavior can be compensated by changing the total bias voltage by less than 80 V. No significant influence of the strong magnetic field on the device timing apart from a small (<0.5 ns) increase of the signal propagation time was observed. The same conclusion holds for both orientations of the axial B-field.

Furthermore, the performance of the two MCP-PMTs with the widest variation in secondary electron yield selected from among the batch of 62 devices with identical mechanical parameters was evaluated in the magnetic field when biased to equal voltage or equal gain. The obtained results emphasize the importance of the SEY dependence of the MCP pores' emissive coating on the electron kinetic energy rather than other parameters such as the total bias voltage.

CRediT authorship contribution statement

Yu.A. Melikyan: Conceptualization, Investigation, Writing - original draft, Visualization. **I.G. Bearden:** Funding acquisition, Writing - review & editing. **E.J. Garcia-Solis:** Funding acquisition, Writing - review & editing. **V.A. Kaplin:** Conceptualization, Writing - review &

editing. **T.L. Karavicheva:** Funding acquisition, Writing - review & editing, Supervision. **J.L. Klay:** Funding acquisition, Writing - review & editing. **T. Marszał:** Funding acquisition. **I.V. Morozov:** Resources. **D.V. Serebryakov:** Resources, Writing - review & editing. **M. Slupecki:** Writing - review & editing, Investigation. **W.H. Trzaska:** Funding acquisition, Writing - review & editing, Project administration.

Declaration of competing interest

The authors declare that they have no known competing financial interests or personal relationships that could have appeared to influence the work reported in this paper.

Acknowledgment

Appendix A. Supplementary data

Supplementary material related to this article can be found online at https://doi.org/10.1016/j.nima.2020.164591.

References

[1] W.H. Trzaska, New fast interaction trigger for ALICE, Nucl. Instrum. Methods A 845 (2017) 463–466.

[2] V.I. Yurevich, et al., Fast Forward Detector Technical Design Report, LHEP/JINR, 2017.

[3] ATLAS collaboration, ATLAS Forward Proton Phase-I upgrade Technical design report, CERN-LHCC-2015-009.

[4] M.W.U. van Dijk, et al., TORCH – a Cherenkov based time-of-flight detector, Nucl. Instrum. Methods A 766 (2014) 118–122.

[5] C. Schwarz, et al., The PANDA DIRC detectors at FAIR, J. Instrum. 12 (2017) C07006.

[6] P. Krizan, Particle identification at Belle II, J. Instrum. 9 (2014) C07018.

[7] G.W. Fraser, The gain, temporal resolution and magnetic-field immunity of microchannel plates, Nucl. Instrum. Methods A 291 (1990) 595–606.

[8] ALICE collaboration, Upgrade of the ALICE experiment: Letter of intent, J. Phys. G: Nucl. Part. Phys. 41 (2014) 087001.

[9] Yu.A. Melikyan, On behalf of the ALICE collaboration, Performance of Planacon MCP-PMT photosensors under extreme working conditions, Nucl. Instrum. Methods A (2019) 61689, http://dx.doi.org/10.1016/j.nima.2018.12.004.

[10] K. Matsuoka, et al., Performance of the MCP-PMT for the Belle II TOP counter, PoS(PhotoDet2015)028.

[11] S. Hirose, Performance of the MCP-PMT for the Belle II TOP counter in a magnetic field, Nucl. Instrum. Methods A 766 (2014) 163–166.

[12] M. Hattawy, et al., Characteristics of fast timing MCP-PMTs in magnetic fields, Nucl. Instrum. Methods A 929 (2019) 84–89.

[13] J. Rieke, et al., Resolution changes of MCP-PMTs in magnetic fields, J. Instrum. 11 (2016) C05002.

[14] S. Korpar, et al., Photonis MCP PMT as a light sensor for the belle II RICH, Nucl. Instrum. Methods A 639 (2011) 162–164.

[15] Y. Ilieva, et al., MCP-PMT studies at the High-B test facility at Jefferson Lab, J. Instrum. 11 (2016) C03061.

[16] K. Inami, et al., Cross-talk suppressed multi-anode MCP-PMT, Nucl. Instrum. Methods A 592 (2008) 247–253.

[17] A. Lehmann, et al., Studies of MCP properties, J. Instrum. 4 (2009) P11024.

[18] N. Kishimoto, et al., Lifetime of MCP-PMT, Nucl. Instrum. Methods A 564 (2006) 204–211.

[19] K. Lung, et al., Characterization of the Hamamatsu R11410-10 3-in. photomultiplier tube for liquid xenon dark matter direct detection experiments, Nucl. Instrum. Methods A 696 (2012) 32–39.

[20] A. Lehmann, et al., Recent progress with microchannel-plate PMTs, Nucl. Instrum. Methods A (2019) http://dx.doi.org/10.1016/j.nima.2019.01.047.

[21] E.V. Antamanova, et al., Anode current saturation of ALD-coated Planacon® MCP-PMTs, J. Instrum. 13 (2018) T09001.

[22] Yu.A. Melikyan, on behalf of ALICE "Light sensors for the Fast Interaction Trigger for the upgrade of ALICE", LHCC 2018 open session.

[23] A.Yu. Barnyakov, et al., Test of microchannel plates in magnetic fields up to 4.5 T, Nucl. Instrum. Methods A 845 (2017) 588–590.

[24] A.Yu. Barnyakov, et al., Microchannel plates phototubes in high magnetic field, J. Instrum. 12 (2017) C09013.

[25] P. Friedag, Setup and Calibration of a Position Sensitive Microchannel Plate Detector and Analysis of a Test Run Optimizing the WITCH Experiment (Dissertation), 2013, p. 27, https://cds.cern.ch/record/1642850/files/CERN-THESIS-2013-250.pdf.

[26] PHOTONIS USA, Inc., Photonis advanced performance microchannel plate, 2018, Datasheet QS22323C-1.

[27] W. Cao, et al., High-sensitivity and long-life microchannel plate processed by atomic layer deposition, Nanoscale Res. Lett. 14 (2019) 153, http://dx.doi.org/10.1186/s11671-019-2983-1.

[28] T.M. Conneely, et al., Extended lifetime MCP-PMTs: Characterization and lifetime measurements of ALD coated microchannel plates, in a sealed photomultiplier tube, Nucl. Instrum. Methods A 732 (2013) 388–391.

[29] V. Ivanov, et al., Numerical simulation of fast photo detectors based on microchannel plates, J. Instrum. 12 (2017) P09024.

[30] P. Chen, et al., Simulation of microchannel plate photomultiplier tube in high magnetic fields, Nucl. Instrum. Methods A (2019) http://dx.doi.org/10.1016/j.nima.2018.10.088.